N·H

ELSEVIER

The MicroGap Chamber: a new detector for the next generation of high energy, high rate experiments

R. Bellazzini *, G. Spandre

INFN-Pisa and University of Pisa, Pisa, Italy

Abstract

The concept of MicroGap Chamber (MGC) is introduced. Results from a large MGC (10×10 cm^2) with a small stereo angle read-out are presented. Both coordinates are read out from the same side of the detector substrate. Measurements of gain stability, fraction of induced charge on the back electrode, uniformity of response along the strip and rate capability have been performed in the laboratory, using X-ray sources. Detection efficiency, spatial resolution, charge and space correlation have been measured with minimum ionizing particle beams at CERN.

1. Introduction

The MicroGap Chamber (MGC) [1] is a new type of position sensitive proportional gas counter made with microelectronics technology. It can be thought of as an ultra-miniaturized version of the MultiWire Proportional Chamber (MWPC), but in a configuration of highly asymmetric anode–cathode gaps. One half-gap has a standard thickness of 2–5 mm, the other has a thickness of only 5–10 μm. The thick gap provides the primary ionization charge, while the ultrathin one is used to very quickly collect the positive charge created during the avalanche process. While in the MWPC the anodes float in the gas, in the MGC they are stuck onto a very thin insulating strip only a few microns wider than the anode microstrip itself. The introduction of the microelectronics technology instead of the iron solder technology in the design and manufacturing of radiation detectors allows the anode pitch to be reduced from the few millimeters typical of the MWPC down to 100–200 μm, and to reach a spatial resolution of a few tens of microns (20–40 μm).

Peculiar to the structure of the MGC is the separation of only a few microns between the anode and the positive-ion-collecting cathode. Due to the large number of field lines ending on the very close back-cathode and to the steep voltage gradient, the process of avalanche charge collection is very fast. About 80% of the total charge is delivered to the preamplifier in 10 ns. In the same time, an almost equal amount of charge is induced on the back-cathode strips. As a result, the rate capability is extremely high ($\sim 10^7$ counts/mm^2 s). The speed of this device is now very close

---

* E-mail bellazzini@pisa.infn.it

to that of solid state detectors. Furthermore, the high electric field which extends over a very small region is not much affected by the anode pitch. This permits an easy design of a detector with variable pitch. The amplifying electric field around the thin-anode microstrip extends over a small volume, but is very intense. It provides gas gains $>10^3$ at 400 V with 14% (FWHM) energy resolution at 5.4 keV.

Another interesting characteristic of the device is its intrinsic 2-dimensional nature. The back-cathode can be suitably structured for the reconstruction of a coordinate not necessarily orthogonal to the anode strips. Radial, stereo or pads structures can be chosen as well.

Due to the good space and time resolution, high rate capability, 2-D capability and considerable flexibility, this device seems very well suited for the instrumentation of tracking systems. It fulfills almost all the stringent requirements of the next generation of experiments (CMS, ATLAS, HERA-B, LHC-B, ALICE) [2–4].

2. The detector

The MGC can be considered as the 3-dimensional evolution of the MicroStrip Gas Chamber (MSGC) [5]). The amplifying electrode structure is no longer in just one plane; use is also made of the third dimension. The anode and cathode are now in two different planes with the insulation between them provided by a thin insulating strip. They can be structured independently, if so desired.

A schematic cross-section of a 2-D MGC is shown in Fig. 1a (not to scale). The figure refers to the so-called "self-aligned" amplification structure [6], obtained with a technology commonly used by the CMOS microelectronics industry. In this technology the anode pattern itself is used as

Silicon substrate 600 μm thick
10 cm x 9 cm (512 anode strips,
256 cathode strips)

read-out of the stereo MGC
50mrad angle (tan α = .05)
schematics of the left sector

Side view   **Top view**

Fig. 1. Cross-section of the double sided stereo MGC.

a mask for the plasma etching of the inter-metal oxide, thus guaranteeing a perfect, built-in alignment of the anode strip with the oxide strip. With this last processing technique, the number of masks needed for the detector construction is reduced to the minimum, i.e. one for the 1-D device and two for the 2-D device. The width of the anode strips is 9 μm at a pitch of 100 or 200 μm. The SiO_2 insulator is 5 μm thick which gives a specific capacitance of ~0.4 pF/cm per anode strip. The choice of the maximum achievable thickness of silicon oxide, from 2 μm in the first generation to 5 μm, allows not only an increased voltage on the cathode strips (with a consequent increase in gain), but the strip capacitance is also reduced, thereby improving the signal-to-noise ratio.

The back-cathode is patterned (80 μm wide strips) with a sampling pitch of 400 μm and at a stereo angle of 50 mrad (Fig. 1b). The substrate is 600 μm thick silicon, passivated with 10 μm of SiO_2. The detector dimension is 10 × 10 cm^2, which is the maximum achievable with the currently available 6 in. wafer technology at the silicon processing foundries. Larger sizes can be nevertheless obtained using as anode–cathode insulator in place of the SiO_2, a thick polyimide film (8–12 μm). A thin layer of a liquid polyimide is deposited by spinning onto a standard glass substrate, on which a metal layer was previously evaporated and patterned (if a 2-D device was requested). Silicon, sapphire, or even plastics or fiber-glass [7] can be used as well. The polyimide is soft-baked at 180°C, then photo-lithographically patterned (by washing in a bath of acetone) and finally hardened at high temperature (~600°C). Because almost no insulating material is left exposed to the gas, there is no need to apply any special treatment to the dielectric to reduce its electrical resistivity and to avoid charging. Requiring neither deposition and etching of silicon oxides nor ion implantation, this technology is quite simple and accessible

to many companies outside the silicon processing world.

Some large area prototypes of such detectors have been already manufactured and tested [8]. A scanning-electron-microscope picture of the internal structure of a MGC at one anode end is shown in Fig. 2. It is possible to recognize the substrate, the cathode (metal 1), the polyimide insulating strip (12 μm thick) and the anode strip (metal 2). The gas filling usually used is pure DME, which has a high cluster density (~60 cluster/cm) and a small diffusion coefficient, or any mixture of DME (70–80%) and CF_4 or CO_2 to increase the drift velocity. Other gas mixtures based on DME and light noble gases (He, Ne) at atmospheric pressure have been recently tested [8,9]. These mixtures allow working at higher voltages, with consequently higher gains. Fig. 3 shows a photo of the signals from anode (upper trace) and cathode (lower trace) strips. The signals have fast-shaping time (~45 ns peaking time) and almost equal amplitudes.
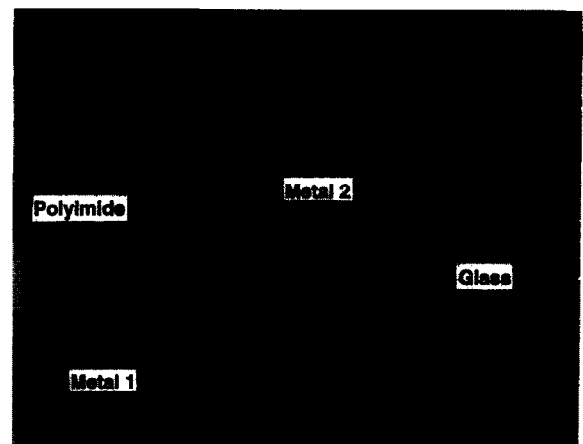
Fig. 2. Photo of the internal structure of the MGC taken with the scanning electron microscope.
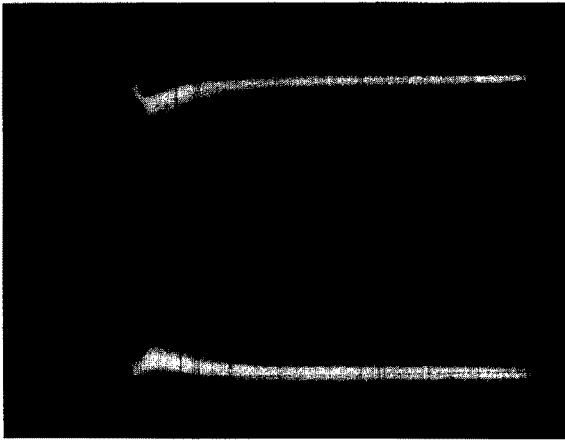
Fig. 3. Anode (upper trace) and cathode (lower trace) signals from the MGC with standard glass substrate (β-source illumination).

Similar signals, but with some difference in amplitude between anode and cathode, have been obtained using detectors with silicon substrate. In that case, there is an effect of the large capacitive coupling of cathode strips to the silicon substrate which reduces the cathode pulse height with respect to the anode pulse height.
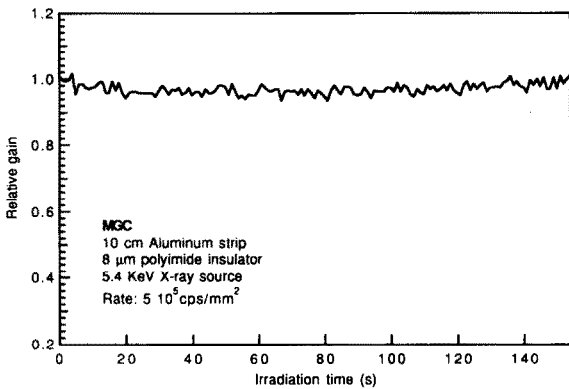
Fig. 4. Short-term measurement of gain stability (charging).
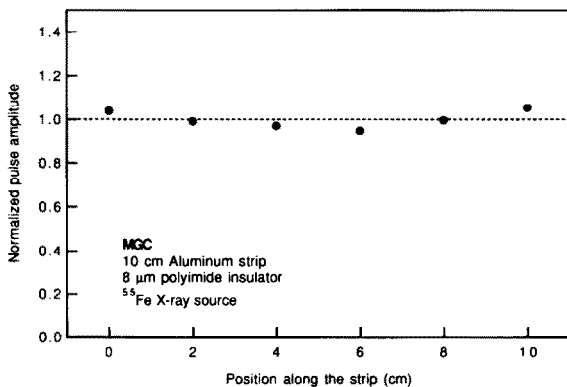
Fig. 5. Uniformity of response along the 10 cm strip.

3. Laboratory tests

Viewing from the top, the MGC is a dielectric free, full metal, device. Charging up is not expected, because there is nothing to charge.

An example of a short-term measurement of the gain stability is shown in Fig. 4. The data refer to a MGC of 10×10 cm^2, with 8 μm thick polyimide film as anode–cathode insulator, aluminum strips and normal glass substrate. The detector was irradiated with 5.4 keV X-rays at a rate of 5×10^5 photons/mm^{2}s. The drift field was $\sim$7 kV/cm and the anode–cathode potential difference was 370 V. Gain variations in the first seconds of exposure were negligible. With the same detector, the uniformity of gain along the strip (10 cm long) was measured using a ^{55}Fe source (Fig. 5). The resulting variations in pulse amplitude were less than 5%.

Aging studies, i.e. long-term measurement of gain stability, have been carried out on a similar device equipped with
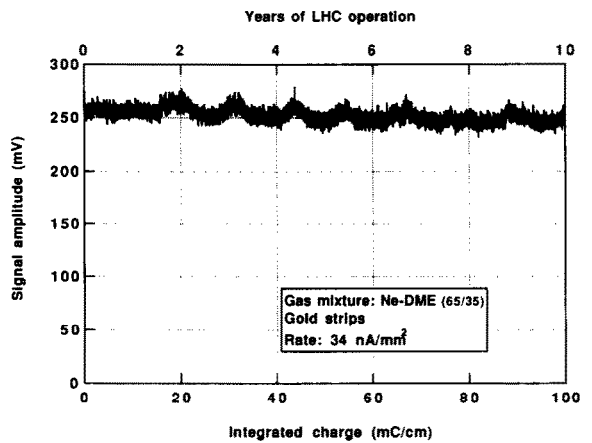
Fig. 6. Long-term measurement of gain stability (aging).
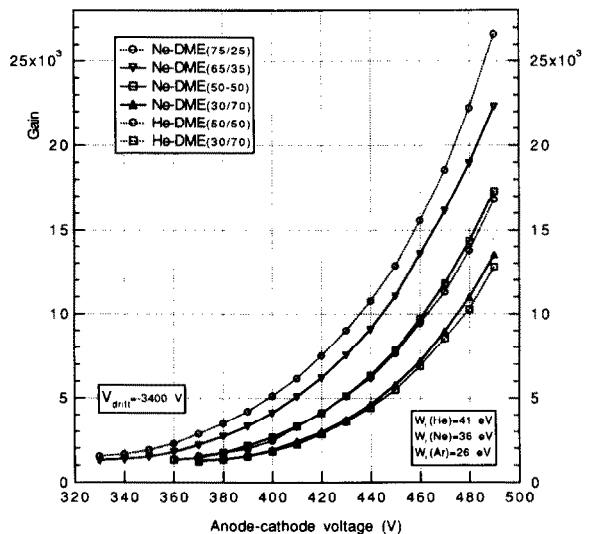
Fig. 7. Dependence of the gain with the anode–cathode voltage for different gas fillings.
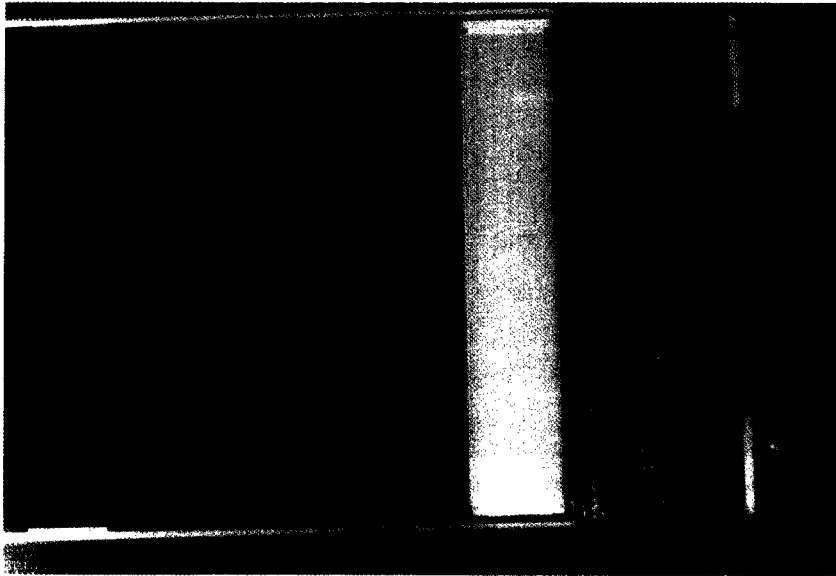
Fig. 8. Photo of the MGC 10×10 cm^2 connected to the front-end electronics.

gold strips. As has been already pointed out in previous papers [10], although use of "very clean" assembly materials and gas system significantly contribute to increasing the lifetime of the detector, from our experience the factor that more strongly affects the ageing is the metallization material of the strips. Chambers with gold strips are much more insensitive to ageing. This is probably due to the fact that gold, being quite inert, is not attacked chemically by reactions with the species produced during the avalanche process.

Fig. 6 shows the detector response during a long-term exposure to a high radiation dose. At a rate of 34 nA/mm^2 from a 5.4 keV X-ray source, no significant variation in gain is observed for an integrated charge of 100 mC/cm, except for a small day–night modulation probably due to differences in pressure and temperature. This corresponds to ≥ 10 years of equivalent LHC operation.

Fig. 7 shows the result of a study of the dependence of gain on the anode–cathode voltage for different gas fillings, based on mixtures of DME and light noble gases (Ne, He). It must be stressed that the large increase in gain, due to the possibility of working at higher voltages, is a property of the gas mixture itself more than the specific MGC design. Indeed, similar results have been obtained with different detector structures.

4. Particle beam tests

Tests were performed with a 300 GeV/c μ^- beam in the H2 line of the SPS North Area and with a 50 GeV/c π^- beam in the X7 line of the PS West Area. In both cases the trigger was the coincidence of scintillator counters which defined a spot of roughly 2×2 cm^2 on the detectors under test. A silicon microstrip telescope was used as external position reference system for track reconstruction.

Three types of devices were tested: two with a size of 10×10 cm^2, made on 600 μm silicon substrate with 5 μm SiO$_2$ as insulator and one with a size of 5×5 cm^2, made on 300 μm standard glass substrate with 10 μm polyimide insulation and gold strips. The two wider chambers differ only in shape: one (MGC$_{10 \times 10S}$) has a square shape with the anode strips parallel to the edges; the other one (MGC$_{10 \times 10W}$) has a wedged shape, with the anode strips at an angular pitch of 0.36 mrad (the pitch ranges from 200 μm at the read-out side, to 170 μm at the opposite side). This wedge detector is a first 2-D prototype for the forward tracker of CMS where the strips have a projective arrangement, pointing toward the beam axis. All the chambers have strips dimension as reported in Fig. 1 and are equipped with stereo strips for a course reconstruction of the second coordinate.

The total number of read-out channels is 768 (512 anode strips and 256 cathode strips) for the larger chambers and 256 anode strips and 128 cathode strips for the smaller one. Both coordinates are read out from the same side of the detector. The front-end electronics, developed by the RD20 collaboration [11], contains a low-noise charge preamplifier and a CR–RC shaper with a time constant of ≈ 45 ns, whose output voltage is sampled and passed to an analogue multiplexer which serializes 128 such channels on a single line. Fig. 8 shows the MGC$_{10 \times 10S}$ and its connection to the front-end electronics.

Each event was reconstructed with a cluster finding algorithm, followed by pattern recognition and fitting procedures. The clustering algorithm requires that each strip in the cluster have $S/N \sim 1.5$–2 and the cluster amplitude be ~ 4–5 times the average noise of a single strip. The alignment of the chambers is done by using iterative fitting pro-

$V_{CATH} = 410$ V – $V_{DRIFT} = 3700$ V – Size 10×9 cm^2
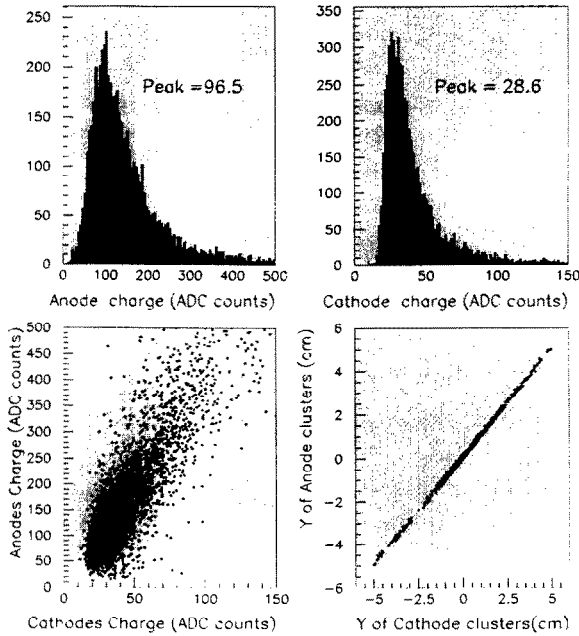
Fig. 9. Landau distributions and anode–cathode correlations for the MGC$_{10 \times 10S}$.

Table 1
Signal-to-noise ratios for all chambers

MGC	S/N_{anode}	$S/N_{cathode}$
MGC$_{10 \times 10S}$	51.4	8.0
MGC$_{10 \times 10W}$	57.9	7.8
MGC$_{5 \times 5}$	~ 30	~ 20

tributions and scatter plots for MGC$_{5 \times 5}$ are shown in Fig. 10. The effect of the signal loss due to the capacitive coupling of the cathode strips to the silicon substrate appears clearly from the ratio $S_c/S_a \sim 1/3$ obtained for the wider chamber. On the contrary, the chamber on glass shows only a small difference in pulse height between anode and cathode ($S_c/S_a \sim 0.8$). Table 1 summarizes the resulting S/N ratios for all the chambers, with the following working conditions: $V_{cathode} = -410$ V, $E_{drift} = -1.2$ kV/mm.

Preliminary results for the position resolution are shown in Fig. 11. The course resolution in X is due to the very small stereo angle (50 mrad). The residual distribution (including the tracking error and multiple scattering) for the r–ϕ projection is $\sigma_{r-\phi} = 42.7$ μm, while the resolution in the r–z projection is $\sigma_{r-z} = 2.3$ mm.

cedures to center the residual distributions.

Fig. 9 shows the Landau distributions relative to the anode and cathode signals obtained with MGC$_{10 \times 10S}$ and their relative correlations in amplitude and space. The same dis-

$V_{CATH} = 410$ V – $V_{DRIFT} = 4000$ V – Size 5×5 cm^2
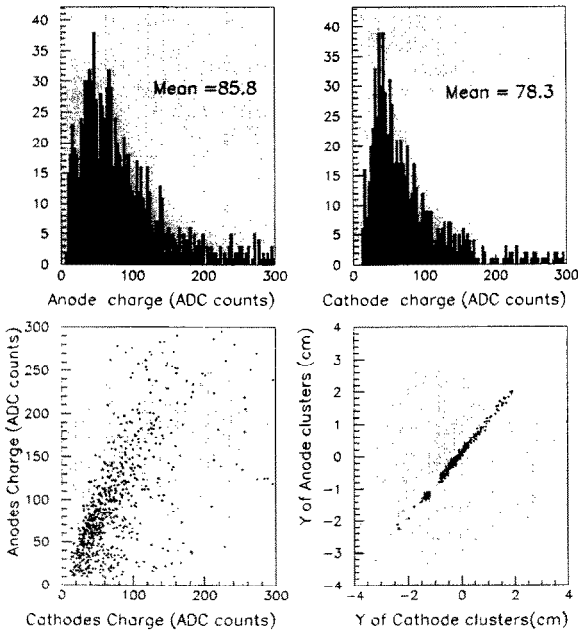
Fig. 10. Landau distributions and anode–cathode correlations for the MGC$_{5 \times 5}$.

$V_{CATH} = 410$ V – $V_{DRIFT} = 3700$ V – Size 10×9 cm^2
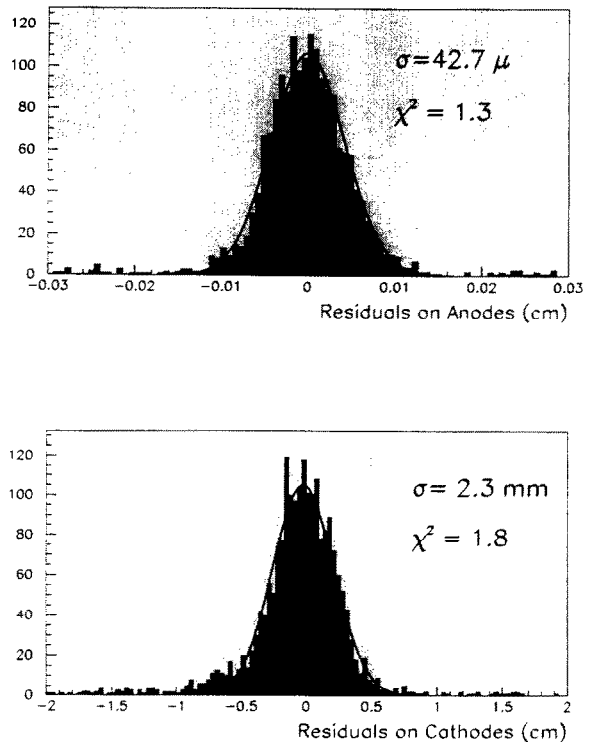
Fig. 11. Residual distributions for both coordinates obtained with the MGC$_{10 \times 10S}$.

5. Conclusions

Even if it is still evolving, the MicroGap Chamber has proven to be a reality. A high gas gain ($>10^3$) can be achieved with structures having very low specific capacitance ($\sim$0.5 pF/cm). Higher gain, well in excess of 10^4, can be achieved by using gas mixtures based on Ne–DME (or He–DME). Full efficiency and good spatial resolution (<40 μm, rms) can be obtained even when operating with very thin gas layers (with a signal to noise ratio well in excess of 50). Furthermore, the development of large area 2-D devices, with performance equal to that obtained with 1-D devices, opens real perspectives to the utilization of the MGC in many applications, including those extremely demanding ones coming from high energy physics experiments.

Acknowledgements

References

[1] F. Angelini et al., Nucl. Instr. and Meth. A 335 (1993) 69.
[2] CMS Collaboration, Technical Proposal, CERN/LHCC 94-38 LHCC/P1 (December 1994).
[3] ATLAS Collaboration, Technical Proposal, CERN/LHCC 94-43 LHCC/P2 (December 1994).
[4] HERA-B, Proposal, DESY-PRC 94/02 (May 1994);
HERA-B, Technical Proposal, DESY-PRC 95/01 (January 1995).
[5] F. Angelini et al., Nucl. Phys. B 23A (1991) 254.
[6] F. Angelini et al., Nucl. Instr. and Meth. A 349 (1994) 412.
[7] J. Moromisato, paper presented at the Int. Workshop on MicroStrip Chambers, Legnaro, Italy, 1994.
[8] F. Angelini et al., INFN PI/AE 95/01, accepted for publication in Nucl. Instr. and Meth.
[9] F. Angelini et al., INFN PI/AE 95/03, accepted for publication in Nucl. Instr. and Meth.
[10] F. Angelini et al., Nucl. Instr. and Meth. A 360 (1995) 22.
[11] RD20 Status report, CERN/DRDC 94-39 (October 1994).